APPLICATION OF AN INTEGRALLY GEARED COMPANDER TO AN SCO$_2$ RECOMPRESSION BRAYTON CYCLE

Jason Wilkes, Ph.D.
Tim Allison, Ph.D.
Joshua Schmitt
Jeffrey Bennett
Southwest Research Institute
San Antonio, TX, USA

Karl Wygant, Ph.D.
Rob Pelton
Werner Bosen
Samsung Techwin
Houston, TX, USA

Dr. Jason Wilkes is a Senior Research Engineer in the Rotating Machinery Dynamics Section at Southwest Research Institute in San Antonio, TX. His experience at SwRI includes design and construction of various test rigs, predicting lateral and torsional rotordynamic analyses, bearings and seals, and auxiliary bearing dynamics following failure of AMB supported turbomachinery. Dr. Wilkes holds a B.S., M.S., and Ph.D. in Mechanical Engineering from Texas A&M University where he studied at the Turbomachinery Laboratory for 6 years.

Dr. Tim Allison is the manager of the Rotating Machinery Dynamics Section at Southwest Research Institute in San Antonio, TX. His research at SwRI includes finite element analysis, modal testing, instrumentation, and performance testing for applications including high-pressure turbomachinery, centrifugal compressors, gas turbines, reciprocating compressor valves, and test rigs for rotordynamics, blade dynamics, and aerodynamic performance. He holds a Ph.D. in Mechanical Engineering from Virginia Polytechnic Institute and State University.

Joshua Schmitt is an engineer at the Southwest Research Institute in San Antonio, Texas. He performs tasks related to the design, evaluation, and analysis of rotating machinery, fluid machinery, and the associated systems. His area of focus has been supercritical carbon dioxide power cycle design and optimization at the system and component levels. Mr. Schmitt graduated from the University of Florida and the University of Central Florida, with a B.S. and an M.S., respectively, in Mechanical Engineering.

Jeffrey A. Bennett is a research engineer in the Pipeline Machinery Simulation group at Southwest Research Institute. His work is primarily focused on the transient modeling of pump and compressor networks, and the development of training simulators. He is also a co-investigator for the design of a linear motor reciprocating hydrogen compressor. Mr. Bennett holds a joint MSc in Turbomachinery Aeromechanics from the Royal Institute of Technology and the Université de Liège. He also holds a BS in mechanical engineering from Virginia Tech.

Dr. Karl Wygant is the Executive Vice President of Engineering for Samsung Techwin's Design and Development Center located in Houston, TX. Dr. Wygant holds an M.S. and Ph.D. in Mechanical Eng-ineering from the University of Virginia and an M.B.A. from Norwich University. His engineering experience over the last 25 years is related to a wide variety of turbomachinery including: rocket-turbopumps, automotive turbochargers, industrial compressors, steam turbines, gas turbines, and novel turbo-machinery applications. His management background incl-udes: project management, multi-group management, business management, and leading

new product development from inception to market delivery.

Robert Pelton is the manager of the development group at the Houston Turbomachinery Design and Development office of Samsung Techwin. He holds a B.S. and M.S. in Mechanical Engineering from Brigham Young University.

Mr. Bosen has over 35 years of experience in the design and manufacturing of turbomachinery. Currently, Mr. Bosen holds a position of Vice President and Executive Chief Engineer at Samsung Techwin America. Previously, Mr. Bosen has worked at various turbomachinery development positions within Linde AG and Atlas Copco. Mr. Bosen has 12 patents on cryogenic expanders, high speed generator sets, and integrally-geared turbomachinery.

ABSTRACT

Integrally geared (IG) compressors, expanders, and companders (combination of expansion and compression stages) are widely used in both air and process gas industries, where the technology has been proven to be reliable and provide increased overall machinery efficiency as compared to barrel-type compressors. The current work describes a novel power block concept for use in a supercritical CO_2 (sCO_2) recompression cycle for concentrating solar power applications. This concept features an integrally-geared compressor-expander, or IG compander (IGC) that allows for reduced cost by utilizing a low-cost, low-speed generator along with compact packaging that can be easily customized for site specific needs. In addition, each pinion may operate at different rotational speeds to optimize performance, and easily allow for inter-stage cooling and expander reheating to further enhance both stage and cycle efficiency.

Because of the close integration of all turbomachinery elements into a single machine, the IGC design optimally lends itself to power block modularization, which makes it suitable for waste heat recovery, fossil fuel power plants, and especially CSP applications. In addition, some range-extension and process control features are more easily implemented in IG compressors and expanders due to their unique and accessible geometry, such as the use of inlet guide vanes, variable-geometry diffuser vanes, and variable-geometry expander nozzles, which present solutions to some of the challenges associated with heat input variation predicted in CSP applications due to varying solar irradiance and power demand.

INTRODUCTION

The primary motivation driving cycle innovation for CSP applications is to further reduce the cost of these renewable systems to be more competitive with traditional fossil fuel plants. The National Renewable Energy Laboratory (NREL) has published extensive assessments of the levelized cost of electricity (LCOE) of CSP. NREL, in cooperation with Sandia National Laboratories, presented an early version of their System Advisor Model (SAM), a renewable energy plant cost model simulator [1]. In that study they modeled both parabolic trough and power tower CSP systems. Using Daggett, California as a reference location for a CSP plant, they predicted that the LCOE of a molten salt power tower with a conventional steam Rankine cycle would reach 9.4 ¢/kWh. Their findings predicted that power towers, with their ability to reach

higher temperatures than parabolic troughs, will achieve higher efficiencies and lower the LCOE [1].

To accelerate the advancement of solar technologies, the U.S. Department of Energy funded the SunShot initiative. NREL published the SunShot Vision Study in 2012, providing more aggressive targets for improving the cost of solar power. The Vision Study suggested that by 2020, the LCOE of a solar power tower could be as low as 6¢/kWh [2]. The study provided targets for key power tower technologies, the solar field, receiver, thermal storage, and power block. Funding was awarded for development of each of these technologies. The Vision Study postulated that achieving a power block with costs as low as $900/kW would require an innovative sCO_2 cycle.

Understanding and implementing the SAM cost model was essential to meet the aggressive goals of the SunShot Vision study. NREL provides detailed documentation with the software, and also produced several publications detailing its financial model, including molten salt power towers [3]. In 2015, the model was updated to include the ability to select a recuperated recompression sCO_2 power block [4]. Within SAM, the performance of the sCO_2 block is based on the published findings of Dyreby et al. [5]. Using this performance estimation, SAM calculates off-design cycle efficiency and estimates the net power output. The behavior of the cycle presented later in this paper may not match the performance predicted by SAM. Once the detailed off-design analysis is conducted, the power generated can be compared to the SAM model predictions, and a new LCOE can be calculated.

Closed loop sCO_2 power cycles offer high energy conversion efficiencies as demonstrated through thermodynamic cycle models. Cycle models offer an efficient means to evaluate a variety of cycle configurations across changing environmental conditions and power demands. The present work builds upon the literature by using established sCO_2 cycle modeling assumptions, and fluid properties from NIST REFPROP.

As established in [6] and [7], the current analysis assumes that optimum recompression cycle performance occurs when the temperature of combining flow streams matches. The present work builds upon this approach by also assuming that the pressure of combined flow streams must be equal. If there is a mismatch in temperature or pressure of combining flow streams, then entropy will be generated and energy lost.

Due to the large variations in heat capacity around the critical point, the present work follows the precedent of [8] by determining heat exchanger performance using enthalpy balances. The more common approach is the Effectiveness-NTU method [9] that uses the minimum heat capacity, which can provide inaccurate results due to the aforementioned variations in the fluid heat capacity.

The present paper improves upon previous sCO_2 power cycle modeling by including pressure drops occurring in heat exchangers, generator losses, and turbomachinery mechanical losses. Target pressure drops in heat exchangers for concentrated solar power applications are in the range of 1-3% [10], which depending on the application may be enough to deter against a second or third stage of inter-heating. Generator losses and turbomachinery mechanical losses can also be significant. By including heat exchanger pressure drops, generator losses and turbomachinery mechanical losses; the present work strives to provide a more complete picture of achievable sCO_2 power cycle efficiencies.

The team of Southwest Research Institute[®] (SwRI[®]) and Samsung Techwin America, a division of Hanwha Techwin (STA), were awarded a project funded by the U.S. Department of Energy SunShot Initiative to develop an IGC for use in concentrated solar power (CSP) supercritical carbon dioxide (sCO_2) plant applications. The current work describes the concept, and illustrates a possible solution to minimize the LCOE and maximize design-point cycle efficiency.

OPTIMIZING THE SYSTEM ADVISOR MODEL (SAM)

The stated goal of the recent APOLLO funding opportunity announcement (FOA) [12] is to develop solar technologies that compete with baseload energy rates, i.e., a levelized cost of electricity (LCOE) of 6 cents per kilowatt-hour or less. To accomplish this, the FOA requires that the LCOE be justified with the SAM software developed by the National Renewable Energy Laboratory (NREL) in collaboration with Sandia National Laboratories. SAM simulates extensive performance and financial information over the lifetime of power plants with renewable energy sources based on system design parameters that are specified as inputs to the model.

Table 1 displays key elements of the cycle design specified in the FOA, and the financial parameters from the SunShot Vision Study (SVS) [2]. These financial parameters were used in the SAM model because they have a direct impact on LCOE, and altering these parameters would not allow for a comparison to previous publications [1-5].

Table 1: Key Parameters Used by the SAM Software

Key Parameters Targeted by FOA		Key Financial Parameters from SunShot	
Design HTF inlet temperature (°C)	720	Inflation rate (%/year)	3
PHX temperature difference (°C)	15	Real discount rate (%/year)	5.5
ITD at design point (°C)	15	Internal rate of return target	15%
Rated cycle conversion efficiency	50%	IRR maturation (years)	30
Power block cost ($/kW)	900	Loan duration (years)	15
Heliostat field cost ($/m^2)	75	Loan percent of total capital cost	60%
Thermal storage cost ($/kWh$_{th}$)	15	Loan annual all-in interest rate	7.1%

Verification of SAM

Before work commenced on this development effort, NETL released version 2015.6.30. This version of SAM includes the capability to model sCO_2 recompression cycles, a feature that was not available when the SunShot Vision Study was performed; this study used a supercritical steam Rankine cycle in place of an sCO_2 recompression cycle. This statement does not imply that the SVS was simulating a steam Rankine cycle, but more so, simulating an sCO_2 cycle with a steam cycle model. Additionally, release 2015.06.30 does not work with the input file from the SunShot vision study, so it was required to recreate the legacy SVS case in the new version of SAM manually. This exercise was done to ensure that no error resulted in converting to the new version of SAM, and allowed the results to be compared directly. The LCOE for these two cases, as shown in Table 2, agree well between the two software versions. Table 2 also shows the LCOE for the SVS inputs when adapted to an sCO_2 cycle type in SAM using the temperature and efficiency targets listed in the APOLLO FOA shown in Table 1. Note that there is a slight increase

in the LCOE for this case relative to the original SunShot Study. This increase is likely due to more accurate cost and performance values when modeling an sCO_2 cycle in SAM using the sCO_2 model over the steam model. All subsequent results in this paper were calculated using the sCO_2 model in SAM with version 2015.6.30.

Table 2: Comparison between SAM Versions and Cycle Types for 200 MW CSP Plant

SAM Version	Cycle Type (in SAM)	Cycle Modeled	Real LCOE ¢/kWh	Nominal LCOE¢/kWh
2014.1.14	Supercritical Steam	Supercritical CO_2	6.14	8.42
2015.6.30	Supercritical Steam	Supercritical CO_2	6.16	8.46
2015.6.30	*Supercritical CO_2	Supercritical CO_2	6.45	8.85

*Inputs merged from SunShot Vision Study with new FOA requirements. Note that the cost of the power block in the vision study has decreased from $1200/kWe to $900/kWe.

Optimization of System Sizing

Since the capacity of the system was not fixed in the APOLLO FOA, the effect of capacity on LCOE was analyzed. To perform this, an sCO_2 system with 14 hours of thermal storage was modeled and the rated capacity was changed. Scale adjustments change the required heliostat field size, receiver height, and tower height. Figure 1 shows the result of a series of the simulations and their impact on the LCOE. There is a noticeable economy of scale demonstrated in the graph that indicates that plants from 50 MW to 200 MW are the most economical; hence, any plant scale outside of that range will have a significant negative impact on LCOE.

Calculations show that a compander unit could be sized up to 25 MW without exceeding current technology limitations. Individually, plants with this capacity would be detrimental to the LCOE; therefore, a power plant using multiple companders to generate energy is recommended to improve the LCOE. Additionally, using multiple units per power plant would cut the cost of the power block and provide redundancy at a reduced cost. To this end, the authors selected two configurations to study; 1) a 100 MW power plant using four 25 MW companders, and 2) a 40 MW power plant using four 10 MW units as the basis for the remainder of this work. This selection was made based on the realization that the first commercial scale plant may be of reduced size to mitigate risk. Additionally, the STEP initiative [13] promises to deliver a 10 MW sCO_2 test facility that could serve as a possible test facility for 10 MW sCO_2 turbomachinery; hence, studying a 10 MW power block has merit.
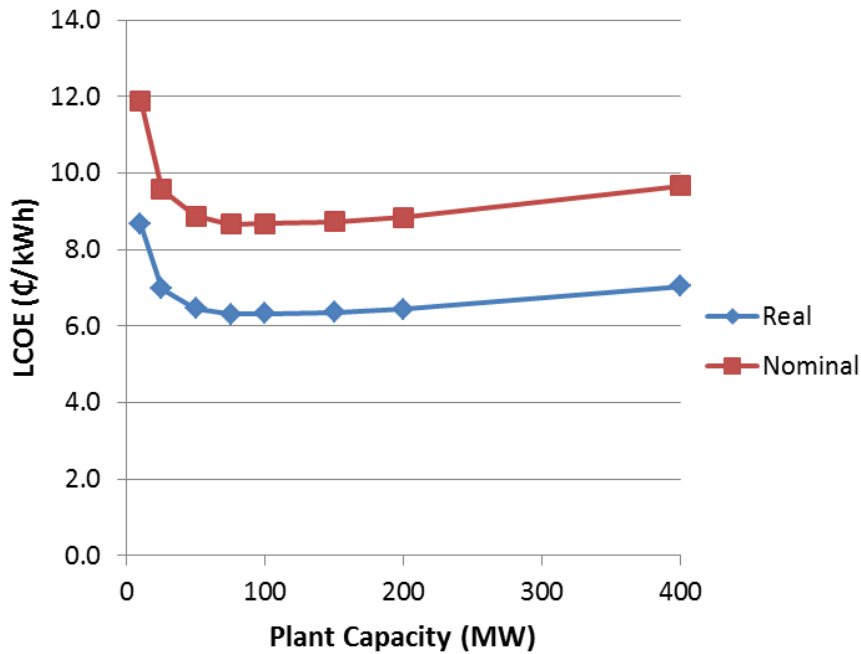
Figure 1: Scale of Plant vs LCOE for an sCO$_2$ Power Tower

Modeling System Alternatives

Having exercised SAM to determine the most appropriate economy of scale for an sCO$_2$ cycle given the APOLLO FOA inputs, the model was revised to reflect the performance of an optimized sCO$_2$ cycle having a compander as the turbomachinery power plant. Although the details of this optimization will be discussed in a subsequent section of the paper, the key results are displayed in Table 3. The ambient temperature, high pressure, and heat transfer fluid (HTF) outlet temperature are all direct inputs into the SAM software, while the low pressure and flow split to the recompressor are factors that affect the efficiency during off-design; SAM does not allow for the direct input of off-design maps to calculate how a system reacts to changes in ambient conditions. The original SunShot model allowed for a wide range of operating conditions, including turbine temperatures above design and power outputs below full load. For this project, the model was changed to limit the turbine inlet temperature to the FOA target. This approach minimizes the material property issues associated with high temperature and maximizes the average power output by the turbine to maintain a favorable LCOE.

Table 3: 50% Cycle Design Parameters Relevant to System Model

Parameters Fixed by Cycle Design	
Ambient temperature at design (°C)	22
High pressure limit (MPa)	27.25
Design HTF outlet temperature from power block (°C)	575.5
Pressure ratio	3.2
Flow split to recompressor	32%

The original SunShot study specified a power tower plant that uses 14 hours of thermal storage, and shuts down after the resource and storage have been exhausted. A 100MW system using this approach was modeled in SAM, resulting in a plant that operates 63.18% of the year with an LCOE of 6.67 ¢/kWh; however, a 40 MW system with similar characteristics has an LCOE of over 7 ¢/kWh. These calculations used power block cost estimates for each plant configuration as detailed in the Cost Estimate section of this paper.

To meet the SVS LCOE target, the option of a fossil fill/backup was introduced into the SAM model. The fossil-fill configuration conceived by the team is as follows: a natural gas-fired heater will be used in parallel with the primary solar receiver to heat the thermal energy storage fluid during when there is insufficient solar-derived energy to maintain the desired turbine inlet temperature. This concept has numerous meritorious benefits. Utilizing fossil-fuel assist helps decrease the LCOE because the capital equipment investment is utilized for a greater percentage of the year. Note that this strategy does not reduce the amount of thermal energy produced, as it only supplements the system when the solar energy is not available. Additionally, utilizing the plant continually reduces start-up and shut-down plant losses, and reduces the number of thermal cycles that ultimately reduces the life of the pressure vessels, turbomachinery, and other equipment.

From this idea, two fossil burning schemes were devised. In the first scheme, fossil fuel is used at all times when solar or stored energy is not available (referred to in this paper as "All Day/All Year" or "Full fill"). Another scheme only burns fossil fuel during periods (1 and 5) where the cost of energy sold to the market is relatively high, as shown in Figure 2. This scheme is referred to as "Daytime/Summer" or "Mix fill". This prevents fuel from being burned at night when it is being sold at lower than the baseline purchase price agreement (PPA), which is less effective in lowering the LCOE. The exception is during the summer, when the thermal storage can last most of the night, and it is beneficial to burn fuel until the solar resource becomes available again to prevent the plant from shutting down.

When SAM simulates the lifetime costs of the plant, it subtracts the cost of annual fuel burned from the plant revenue. Natural gas was selected as the fuel to be burned for fossil assist, and a price of $2.75 per MMBTU was input based on forecasted natural gas prices [11]. The results of a few options that include fossil fill and a 100 MW plant without fossil fuel assist are reported in Table 4. The 40 MW plant requires full-fill to reach the desired LCOE, running 99.69% of the year. However, 66.10% of the energy this plant produces comes from fossil, not solar. Larger 100 MW plants with full fossil fill achieve an LCOE much lower than 6 ¢/kWh, but, again, a large portion of its energy comes from fossil fuels. In contrast, a mixed fossil fill scheme 100 MW plant with 12 hours of thermal storage is able to hit the target LCOE, operating for 74.16% of the year with only 18.09% of its power coming from a fossil source. Once again, all three of these 100 MW plants configurations produce the same amount of solar energy during the year; however, the plants utilizing fossil assist are utilized for a greater percentage of the year, allowing the fossil fueled energy to help pay for the capital expenses of the plant. This ultimately lowers the LCOE.

For implementing a natural-gas-fired option, one factor that must be considered is a future tax on carbon dioxide emissions. In order to estimate the CO_2 emitted from each plant, the annual natural gas use was recorded from each SAM simulation in millions of BTUs. This was multiplied by the emission coefficient reported by the U.S. Energy Information

Administration [15], and then divided by the annual generation. The results for fuel use and CO_2 emission per MWh generated are presented in Table 4. As expected, the case with a mixed use of fossil produces the least amount of carbon dioxide emissions per MWh generated. Logically, the inclusion of thermal storage also reduces the annual emissions.
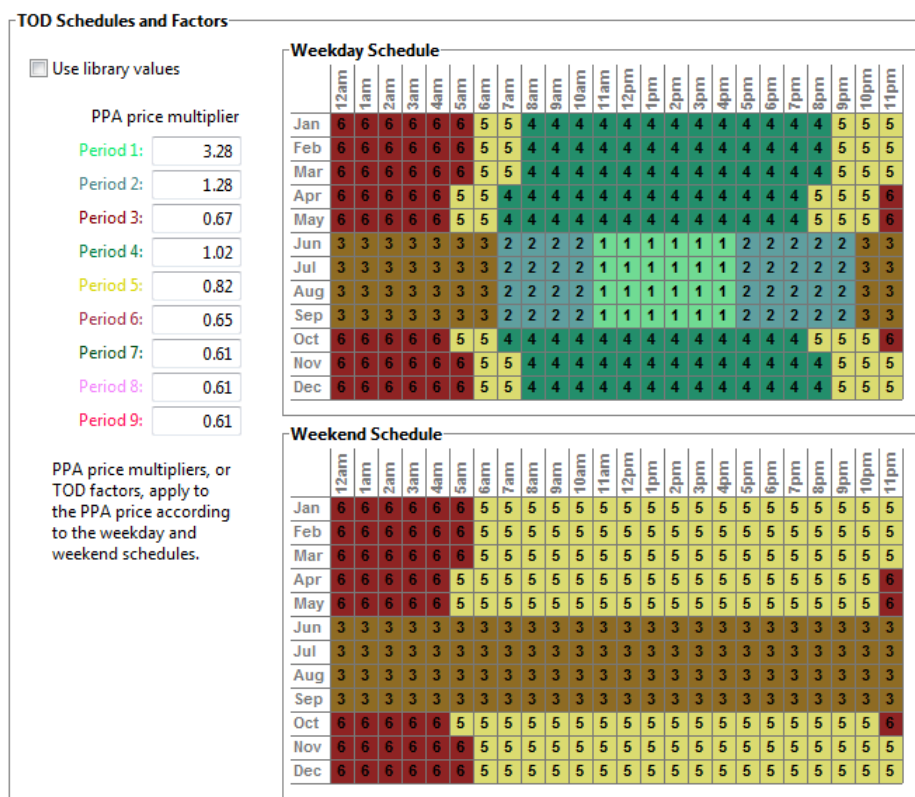
Figure 2: Schedules for Time of Delivery and Corresponding Price Multipliers

Table 4: Investigated System Models

Size (MW)	100	40	100	100
Annual generation (MWh)	768,037	310,815	550,754	454,993
Annual operation time	99.87%	99.69%	74.16%	63.18%
Percent power from fossil	36.52%	66.10%	18.09%	0.00%
Thermal storage (hrs)	12	0	12	14
Fossil fill	All Day/All Year	All Day/All Year	Daytime/Summer	None
Fossil backup cost ($/kW)	50	50	50	0
Power block cost ($/kW)	800	925	800	800
Real LCOE (¢/kWh)	4.95	5.90	6.00	6.67
Nominal LCOE (¢/kWh)	6.80	8.10	8.24	9.16
Annual fuel use (MMBTU)	1,899,547	562,362	966,168	0
Annual CO_2 emitted (kg/MWh)	181.5	328.0	93.0	0
Average Ambient Temp. (°C)	19.9	19.9	22.9	23.4

The average ambient temperature, also tabulated for each case, affects the target design point cycle efficiency. According to our cycle optimization, an average ambient of 22°C achieved a 50% efficient cycle. When the off-design performance of the optimized cycle is modeled, this will be checked for conformance to the SAM model's response to changing ambient conditions.

When predicting future costs of generating electricity with fossil fuels, an imposed cost of CO_2 emission should be considered. The cost of carbon can depend on the market cost of carbon trading, CO_2 emission taxes, or some combination of both. The effect of a carbon tax on LCOE is demonstrated in Figure 3 for each of the four simulated CSP power plants contained in Table 4. The carbon cost is assumed to match the inflation rate over the 30 years simulated. Also included in the figure are several example carbon taxes for countries around the world [16]. Note that these carbon taxes are based on rates applied to industry, not rates charged to individuals. For countries that use a carbon trading market, the cost of carbon can fluctuate. It reached as high as $142/Tonne on the Tokyo market when it opened in 2010 [16]. The system model that does not include fossil fuel is also shown in Figure 3. This serves as a baseline that demonstrates where the fossil burning plants have a higher real LCOE due to the cost of carbon emissions. These results show that even with typical current carbon costs, numerous fossil-fill schemes can be selected to keep the LCOE below 6¢/kWh.
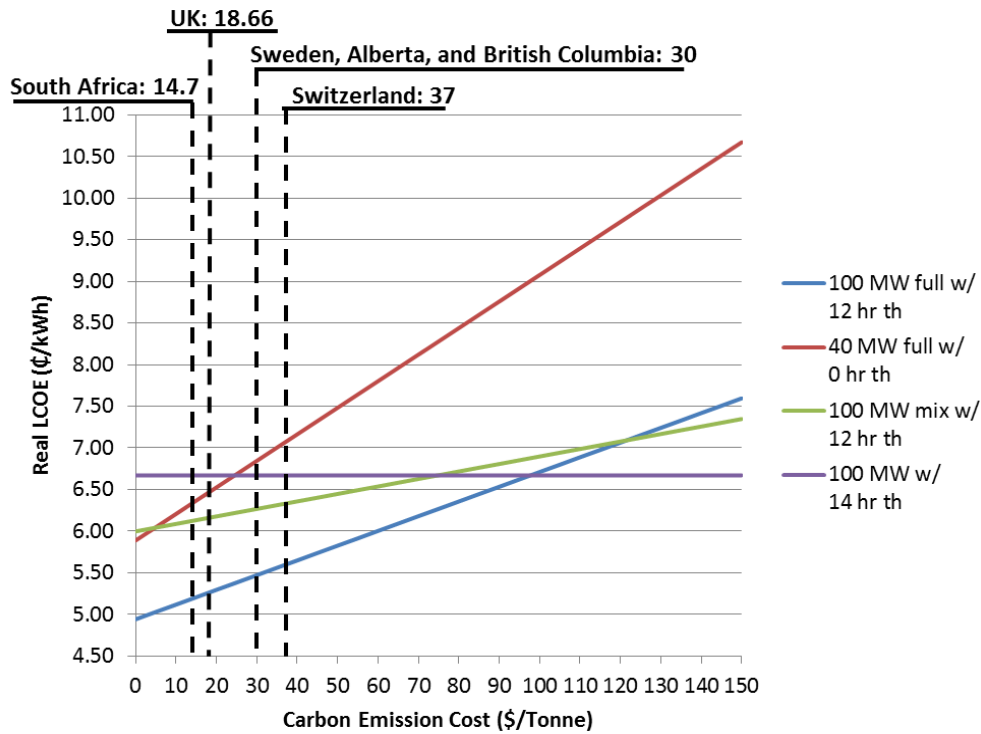
Figure 3: Real LCOE trends for changes in carbon cost

Levelized Cost of Electricity Breakdown

In order to illustrate the distribution of money within the LCOE, the individual costs were categorized and organized into the charts shown in Figure 4 and Figure 5.
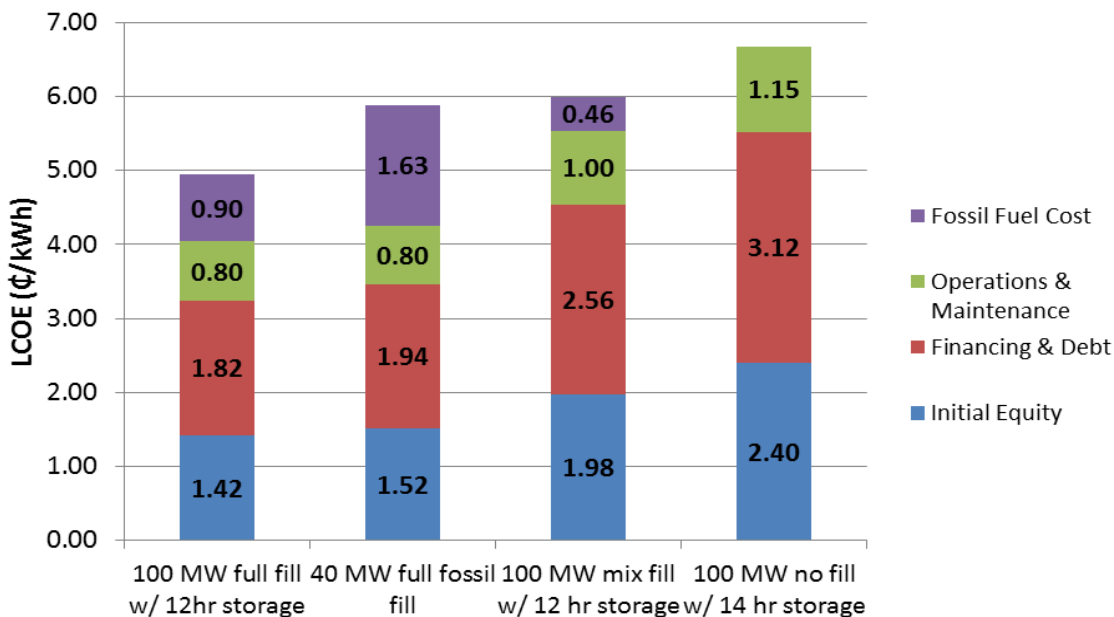
Figure 4: LCOE Breakdown by Expense Type
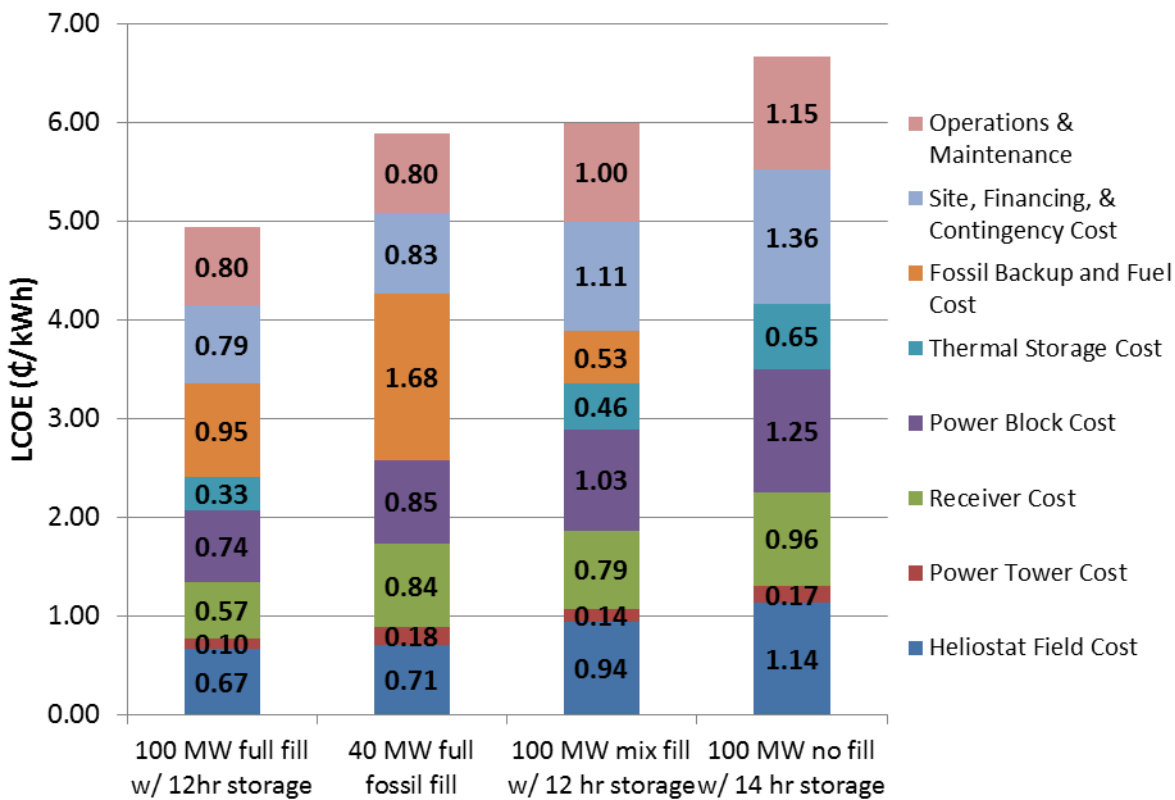
Figure 5: LCOE Breakdown by System Cost

Figure 4 illustrates how the upfront charges and debt dominate the cost of electricity. As more fuel is burned, the plant sells more electricity. This brings down the levelized cost overall,

but the annual costs of fuel and of maintenance become larger factors. The impact of each component of the plant is shown in Figure 5. Of the individual components that are initial costs, the power block is the largest contributor to capital cost, even with the cost savings provided by the compander system. The heliostat field is another major contributor to the capital cost of the plant. On the tower, the receiver is a much larger cost compared to the construction of the tower itself. The mix fossil fill scheme shows how thermal storage can help reduce fuel consumption costs compared to the full fossil fill.

COST ESTIMATION

To assist in the process of identifying an optimal approach in the design of the turbomachinery for CSP applications, cost models of various sized power blocks were developed. At this time, the models are benchmarked against known costs to the maximum extent possible. As the turbomachinery design matures and additional information becomes available for critical components, the cost model will be updated accordingly.

Power Block Cost Components

To estimate the cost of various power block sizes and configurations, a "cost model" was produced. The cost model incorporates cost estimates of the various components:

- Enclosure for Power Block (PB)
- Power Conditioning Components: Generator, Switching Gear, and Transformer
- Instrumentation and Controls
- Compressor Expander "Core Turbomachinery"
- Recuperators (High-Temperature and Low-Temperature)
- Expander Re-heater
- Compressor Intercooler
- Piping and Insulation
- Installation and Commissioning Cost
- Contingency

The top five material related cost drivers are expected to be, in order of highest to lowest capital expense: 1) turbomachinery, 2) high-temperature (HT) recuperator, 3) low-temperature (LT) recuperator, 4) re-heater, and 5) generator. The cost models for these components are explained in greater detail in the following sections.

Turbomachinery Core

Figure 6 shows the estimated turbomachinery cost per generator power output (specific cost) for the CSP owner to buy the turbomachinery plotted relative to generator power. The turbomachinery portion includes the following: expansion and compression stages, bull gears, pinions, bearings, seals, volutes, collectors, coupling, and gear housing; in essence, all the turbomachinery components associated with compression and expansion. The model is benchmarked in two ways: components and entire units. Component-based estimates are also used that individually estimate the cost of each component for the specific CSP application (five

cases chosen: 1MW, 5MW, 10MW, 20MW, and 30MW.) Four reference cases that are high-pressure gas compressors are scaled to take into consideration higher strength alloys to handle the high pressure and temperature. From these two separate approaches, a curve fit model is applied to estimate turbomachinery costs. Notice the substantial decrease in cost as generator power increases from 1MW to 7.5MW. Above 7.5MW, some savings are also present, but the level of savings is reduced. As the design process matures, it will become possible to receive quotes for each component and build an improved cost model.
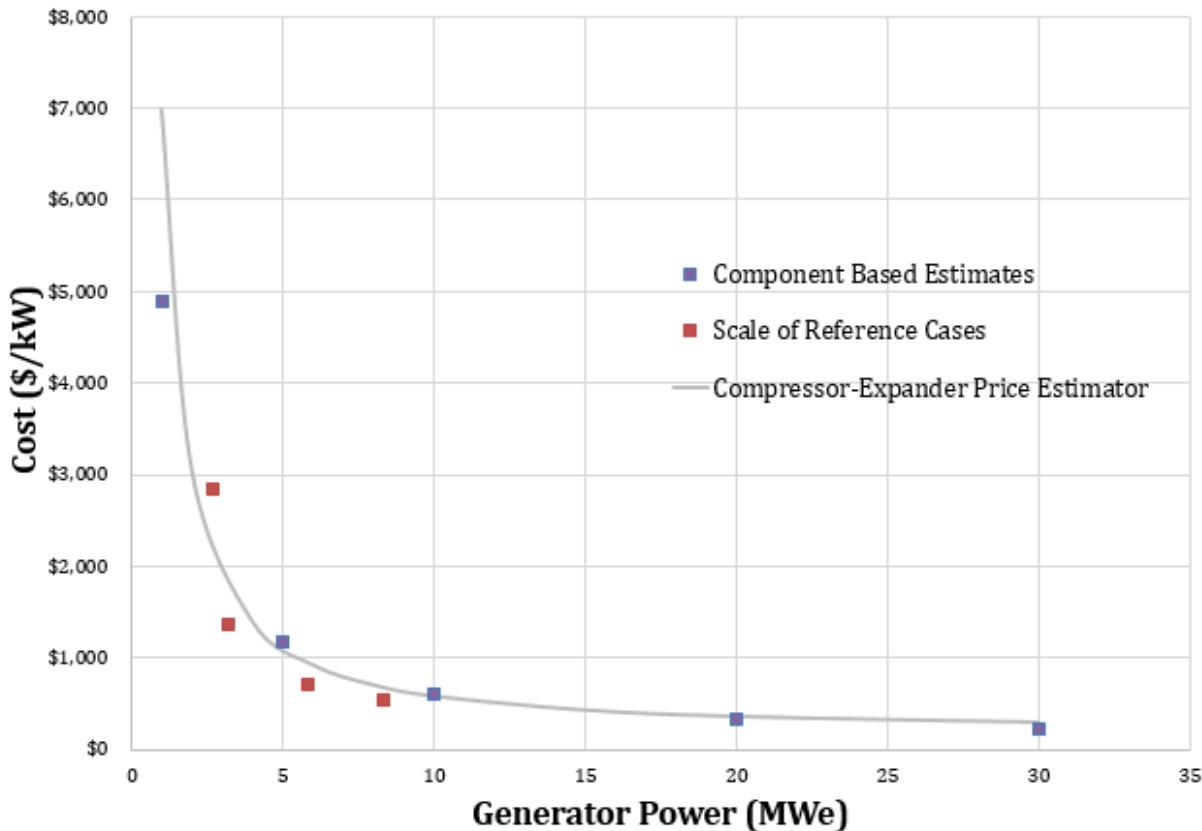
Figure 6: Cost Estimation for turbomachinery portion of Power Block

Recuperator and Re-heater Cost Models

Costs for the recuperators and re-heaters are expected to be strong cost drivers for the entire power block. Table 5 lists the cost models applied. These cost models are based upon extrapolation from a single-point reference for the high-temperature recuperator presented at the 2015 Electrical Power Research Institute (EPRI) conference [10]. The costs for other heat exchangers are reduced due to lower operating temperatures and pressures of one or both streams. The costs are assumed to vary in a linear fashion to the thermal power as estimated in Table 1.

Table 5: Cost estimates for the various heat exchangers expected in the cycle

Component	Duty Estimation ($kW_{Thermal}/kW_{Generator}$)	Cost Estimation ($\$/kW_{Thermal}$)
High-Temperature Recuperator	3.990	50
Low-Temperature Recuperator	1.269	30
Primary Heater & Re-Heater	0.983	40
Cooler	0.983	25

Generator

Figure 7 shows the cost model applied for estimating the capital cost of the generator for the CSP owner. Generator power is shown along the horizontal axis with the vertical axis showing the cost divided by kW delivered. The cost model is shown as a solid line that is benchmarked by actual generator quotes for six different cases. The capital costs decrease substantially relative to reducing the power from 1MW to 10MW. Additional relative cost reduction is possible above 10MW.
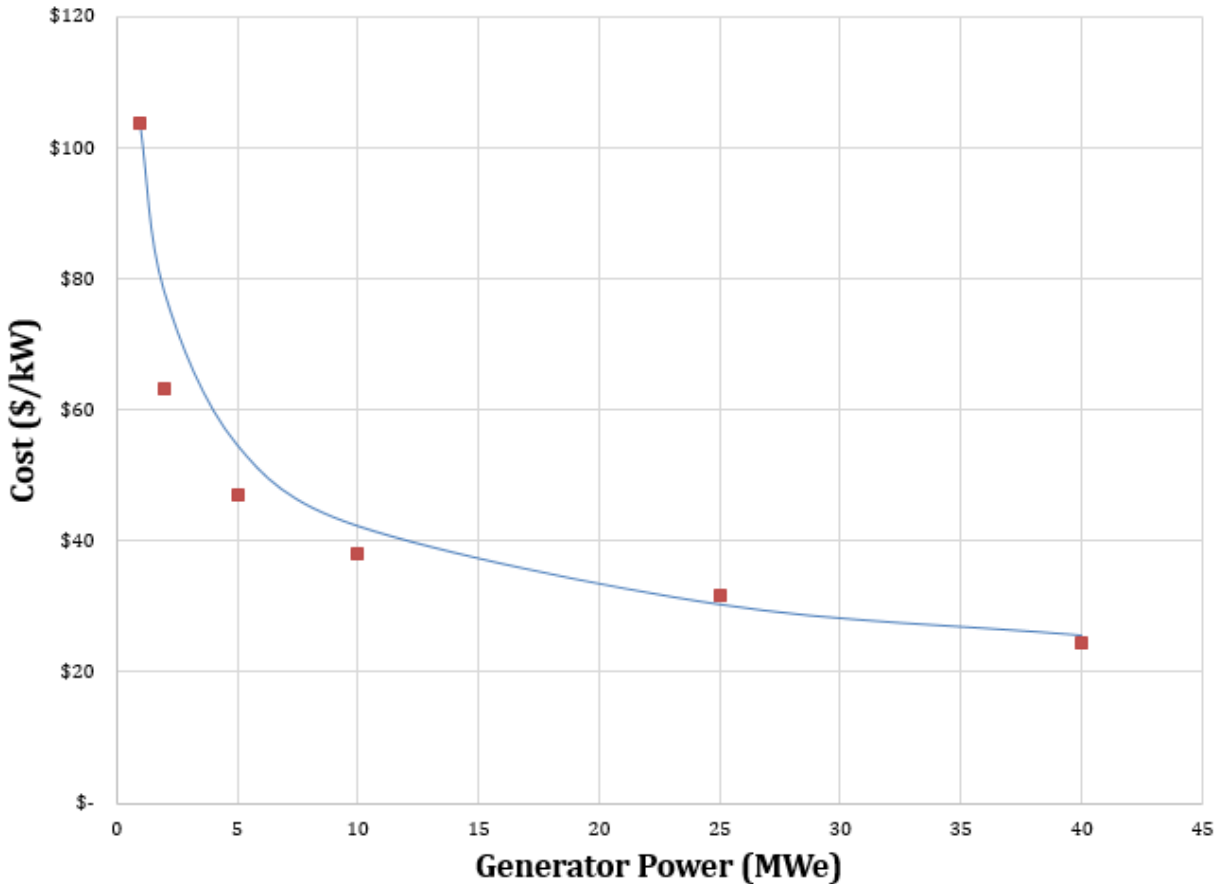
Figure 7: Cost model for generator

Other Relevant Cost Models

Table 3 shows the models applied for other significant cost items. A 50% escalation is applied for multiple units for the enclosure and installation and controls system. In other words, two identical units would cost in total 1.5 times a single unit, three identical units would cost 2.0 times a single unit, and so on. The enclosure is expected to be an uninsulated steel structure with self-enclosed ventilation and no acoustic treatment applied. The instrumentation and controls are expected to be related to operational equipment health: critical temperatures, critical pressure locations, flow, and surge related control.

Table 6: Cost Models of other sizable components to the CSP IG compressor-Expander Recompression Brayton Cycle

Component	Cost Model
Enclosure	$175,000
Instrumentation and Controls	$350,000
Switching gear/transformer	25% generator/ 20% generator
High Temperature Piping	$72/kg
High Temperature Insulation	$105/kg
Installation and Commissioning	10% of PB components (excluding piping and insulation)
Contingency	5% of PB components 0% enclosure 0% Installation and Commissioning)

Power Block

Figure 8 shows the total estimated capital expenditure by a CSP owner for the power block of the integrally-geared recompression Brayton cycle, based upon the aforementioned cost models. Along the horizontal axis is the delivered power and along the vertical axis is the specific power block cost. Several options are provided. Multiple power block cycles can be operated in parallel for several reasons. First, with multiple units operating in parallel, the non-recurring engineering cost of the turbomachinery may be spread to multiple units. Also, savings from buying multiple components may be applied. Savings for acquiring multiple generators are estimated at 2% per each additional generator. Also, in operating multiple units, it becomes possible for a CSP owner to add reliability margin by purchasing three units, operating two and keeping one unit as a spare. Integrally-geared units of 40MW, 50MW, and 60MW are also achievable in the future, but due to current manufacturing limitations, these may not immediately be available. Meeting DOE price target estimates of less than $900/kW appears to be achievable for ranges of 15MW to 120MW, with growth potential for larger applications and lowering power block cost per kW.
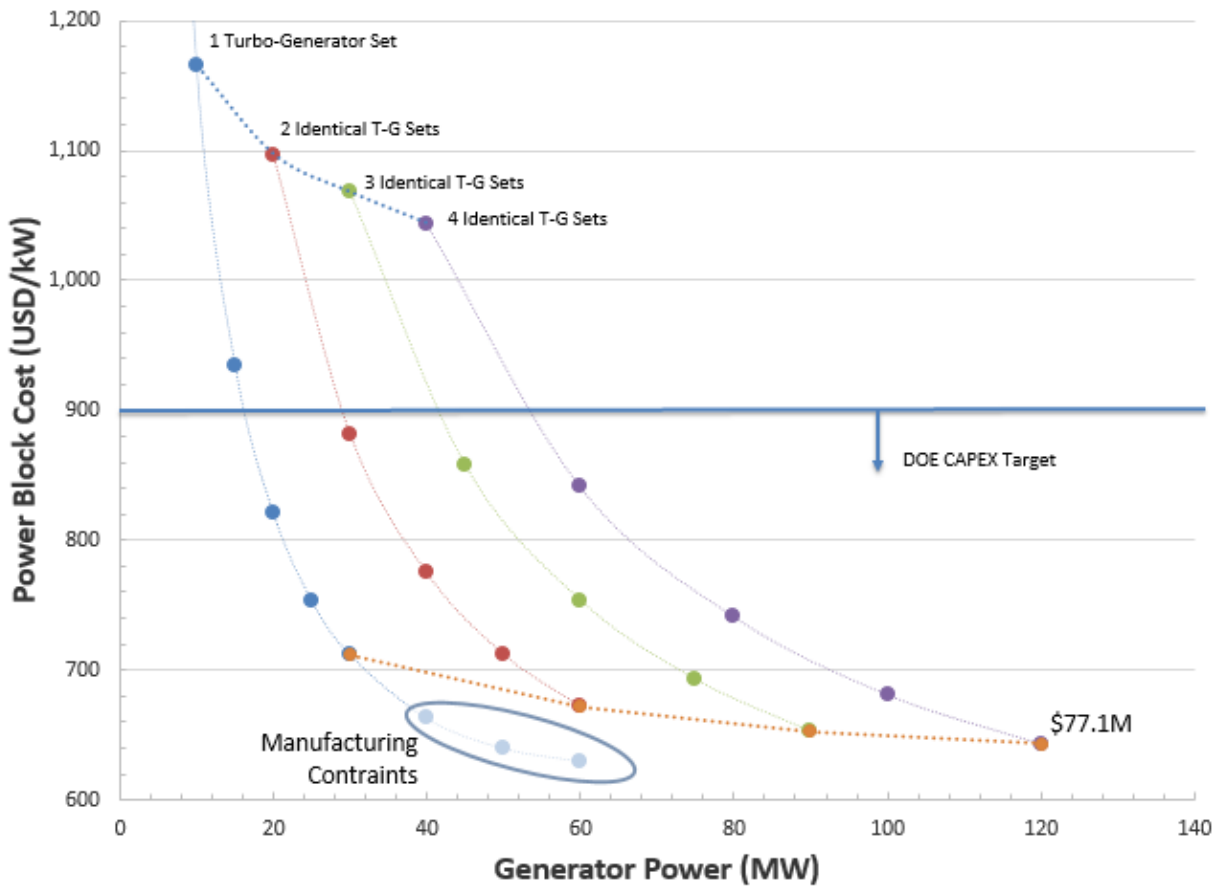
Figure 8: Cost estimate of the power block for CSP systems

CYCLE OPTIMIZATION

This section details the optimization process used to achieve the best possible efficiency with an sCO_2 cycle utilizing an IGC as the power block. The target for this optimization as specified in the APOLLO FOA was 50%. At this point in the development effort, the cycle calculations have focused on design point estimations of cycle efficiency; that is, the reduction in efficiency as the compressor/turbine are operated off-design has not been thoroughly investigated. This will be the subject of future work. For this analysis, the power block efficiency is defined as the ratio of the work output through the generator, as electricity, to the heat added to the cycle; thus, it accounts for turbomachinery, recuperator, and generator efficiencies, as well as pressure losses in heat exchangers.

Cycle modeling was performed using Numerical Propulsion System Simulation (NPSS) [16], an established thermodynamic tool commonly used in the air breathing engine industry. NPSS was selected for its ability to quickly perform system design parameter sweeps. NPSS was linked to National Institute of Standards and Technology (NIST) Reference Fluid Properties (REFPROP) [18] to provide accurate fluid properties of CO_2. As established in the literature, notably [7] and [8], recompression cycle designs are often constrained such that the temperature must match when flow streams recombine. Additionally, cycle models were

constrained such that the combination of flow streams occurred at equal pressures to prevent losses. To verify the NPSS cycle modeling approach, a comparison was performed with the recompression cycle with intermediate re-heat used in [7], and it was found that the predicted cycle efficiencies matched within 0.04%.

The wide-range integrally-geared (WRIG) Compander project focuses on the design of unique turbomachinery; however, there are many other components to consider when modeling an sCO$_2$ cycle. Therefore, a literature review was conducted to find realistic pressure limitations for state-of-the-art heat exchangers, recuperators, and piping. Another constraint was the decision to keep the CO$_2$ in the supercritical region throughout the recompression cycle. The results of the literature review were combined with aggressive turbomachinery efficiency targets to determine appropriate model inputs that have been summarized in Table 7. While this research constrained many facets of the cycle, a number of design choices remained, including (1) the use of intercooling and/or inter-heating, (2) the selection of cycle pressure ratio, and (3) the percentage of flow split between the main compressor and re-compressor.

Table 7: Cycle Model Inputs

Group	Property	Value
Heat Exchanger	Pressure Drop (each Heat Exchanger)	1 %
	High Temp Recuperator Effectiveness	97 %
	Minimum Pinch Temperature	5 °C
	Heater Outlet Temperature	705 °C
	Cooler Outlet Temperature Range	35-55°C
Generator and Mechanical Efficiencies	Generator Efficiency	98.7%
	Compressor Mechanical/Pinion Losses	4%
	Turbine Mechanical/Pinion Losses	2%
Pressure Limits	System Min Pressure	1,070 psia
	System Max Pressure	3,953 psia
Turbomachinery	Compressor Isentropic Efficiency	83.5%
	Re-Compressor Isentropic Efficiency	84%
	Turbine Isentropic Efficiency	92%

The WRIG compander design is unique in that the two main compressor stages and four turbine stages are physically separated from one another, thus, intercooling and inter-heating is more natural to incorporate into the design. A schematic of the cycle with all possible re-heat and intercooling stages is shown in Figure 9. To determine which configurations of intercooling and inter-heating would be most advantageous, eight cycle configurations were simulated across a variety of flow splits and pressure ratios for a constant compressor inlet temperature. Another factor considered for the intercooling scenarios was the amount of compression handled by the first and second stages. The best efficiencies of this study as a function of pressure ratio are shown in Figure 10.
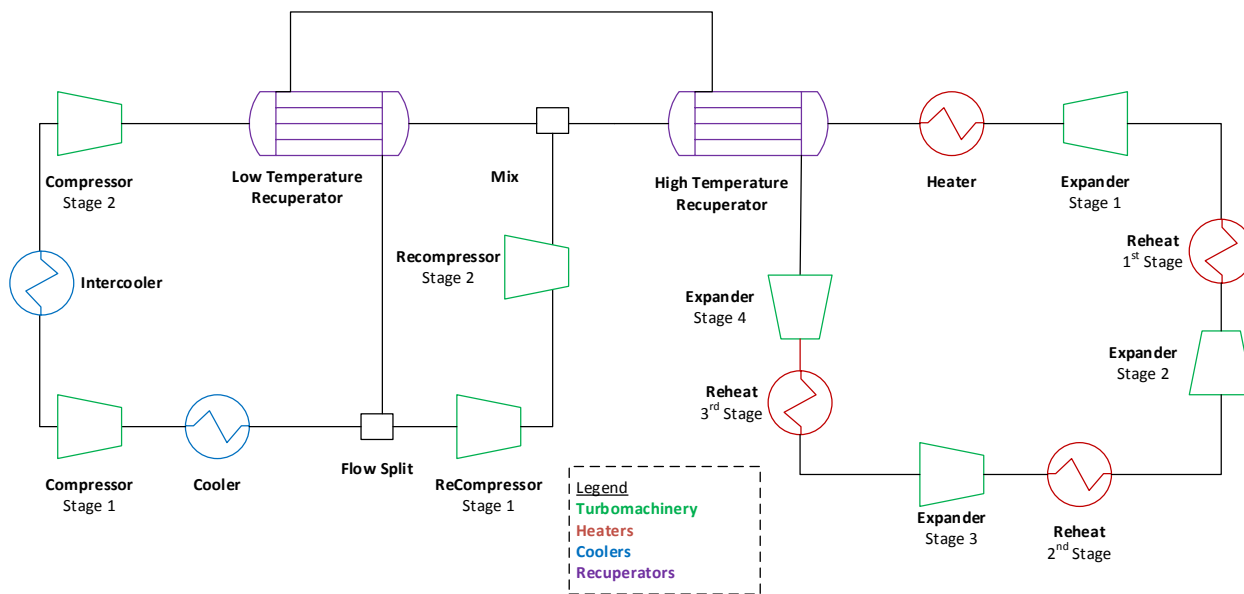
Figure 9: Cycle Schematic Shown with all possible Intercooling and Inter-heating Options
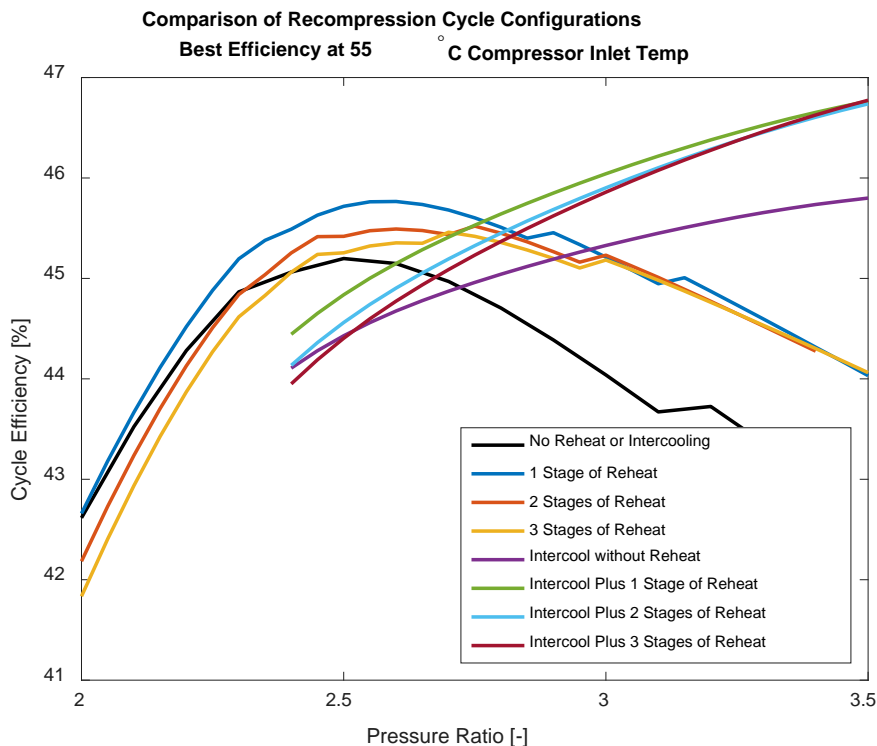
Figure 10: Comparison of Re-heat/Intercool Options at 55°C Inlet Temperature

The results show two groups of curves. The first group, denoted by efficiencies peaking near a pressure ratio of 2.5, do not have intercooling. The best efficiency in this group is the configuration with one stage of re-heat that is located between the second and third expansion stages. Additional stages of re-heat may increase the power output of the cycle, but due to the additional pressure losses caused by including more heat exchangers, the cycle efficiency does

not benefit. The second group that is noted by efficiencies increasing up to a pressure ratio of 3.5, which was the limit of this study, has compressor intercooling. With increased piping strengths, there may be additional realizable configurations with intercooling above pressure ratios of 3.5; however, these were not considered in this study. Similar to the first group, one stage of re-heat offers the highest efficiency, on the order of 0.5% to 1% gain relative to configurations that do not have turbine reheating.

The previous study found two distinct cycle configurations that had promising efficiencies, a single stage of turbine reheat between the second and third stage with and without intercooling. These configurations were then optimized at various inlet temperatures to determine the best efficiency point for the cycle as a function of compressor inlet temperature, pressure ratio, and flow split. The best efficiency points for each compressor inlet temperature are shown in Figure 11. As expected, lower compressor inlet temperatures correspond with generally higher cycle efficiencies. These results show that an efficiency of 50% is achievable for the configuration with one stage of re-heat with and without intercooling at 36.5°C and 39.6°C, respectively. These temperatures are near the average temperature expected at the inlet of the compressor throughout the year as shown in Table 4; therefore, it seems to be a reasonable choice for the cycle design point. At higher compressor inlet temperatures, intercooling has the advantage, while at lower temperatures it does not. The flow split for intercooling remains close to 32% mass flow to the recompressor while the configuration without intercooling diverts increasingly more flow to the recompressor as the compressor inlet temperature decreases.

Figure 11 shows the challenge in maintaining optimal cycle efficiencies as the inlet temperature to the compressor varies. Consider operating in the afternoon with an inlet temperature of 50°C (denoted by point A on the figures). At this time, running with a pressure ratio of 3.5 with compressor intercooling and one stage of re-heat provides the best efficiency. As the temperature of the ambient air decreases, eventually settling at a compressor temperature of 40°C, the plant will have to switch from the compressor intercooling to a configuration without intercooling at a pressure ratio of 3 to maintain maximum cycle efficiency. This configuration would result in less dense gas at the inlet of the compressor and recompressor. Additionally, the ideal flow split shifted from 32% to 28%, further increasing the compressor actual flow. This scenario shows the challenge of maintaining high compressor efficiency with changing ambient air temperature.
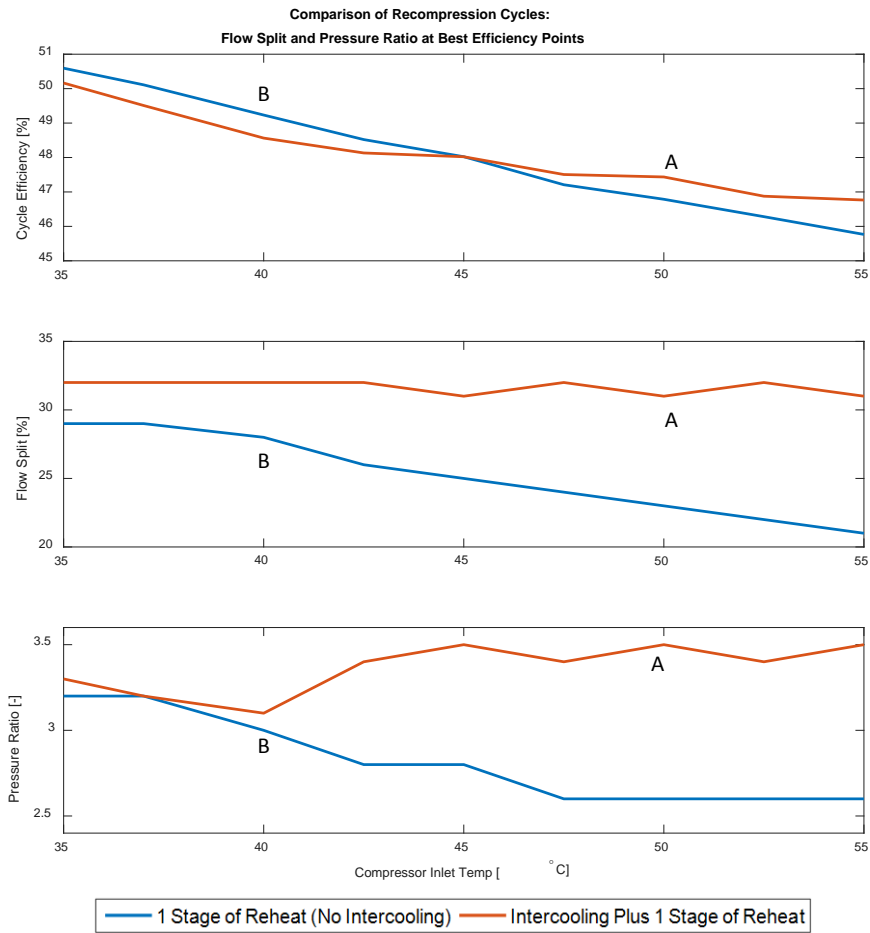
Figure 11: Flow Split and Pressure Ratio of Maximum Efficiency Point against Compressor Inlet Temperature

TURBOMACHINERY OVERVIEW

An integrally-geared compander integrates the required turbine and compressor units into a single package based around a large speed-increasing gearbox coupled to a conventional low-speed electric generator. A four-pinion machine, consisting of two lower-speed shafts for the turbines, and two higher-speed shafts for the compressors is envisioned to match the cycle conditions shown in Table 7. The pinons will be driven at different speeds to minimize stage count (cost) and maximize efficiency (power production). A modular design approach is proposed to produce a basic frame design that can be easily matched to a wide range of process conditions. This is possible since the individual turbine and compressor stages are mounted on separate pinions attached to the common gearbox. By scaling the individual stages, the compander can be modified to match a wide range of powers using the same validated mechanical design.

For this project, an SE110-class gearbox will be used. This has an approximate center line distance of 1,100 mm and can accommodate stages up to 900 mm in diameter. The maximum size is limited by the physical constraints of the gearbox and mechanical limits of the gears and bearings. The minimum size is limited by rotordynamic constraints, which develop as

the pinion speeds increase. For sCO$_2$ applications, the SE110 gearbox is being evaluated to cover a potential range of 5 to 25MW; however, these units can be coupled together to constitute the power block for a larger overall system. The mechanical design of the system will be confirmed at the largest flow (highest power) condition of the gearbox. In cases where less heat is available, smaller, lower-flow compressors and turbines can be used in place of the full-scale, high-power, configuration.

Frame Capabilities

Figure 12 shows the preliminary design of the turbomachinery core, turbines, and compressors sized for a range of power production from 5 to 25MWe.
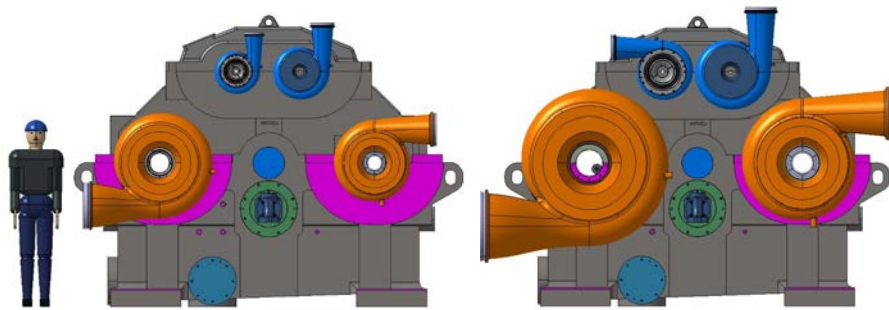
Figure 12: SE110 Core Configured for 5MWe (left) and 25MWe (right)

Preliminary performance estimates show that the turbomachinery core is most efficient when applied at the maximum flow and power conditions. Figure 13 shows how the efficiency of both the turbine and compressor sections increase with increasing power. This increase in efficiency is due to aerodynamic performance gains associated with scaling the turbines and compressors to larger sizes. The percentage of mechanical losses from the gears and bearings are also less significant at higher powers. These numbers are included in the cycle and system analysis results described previously.
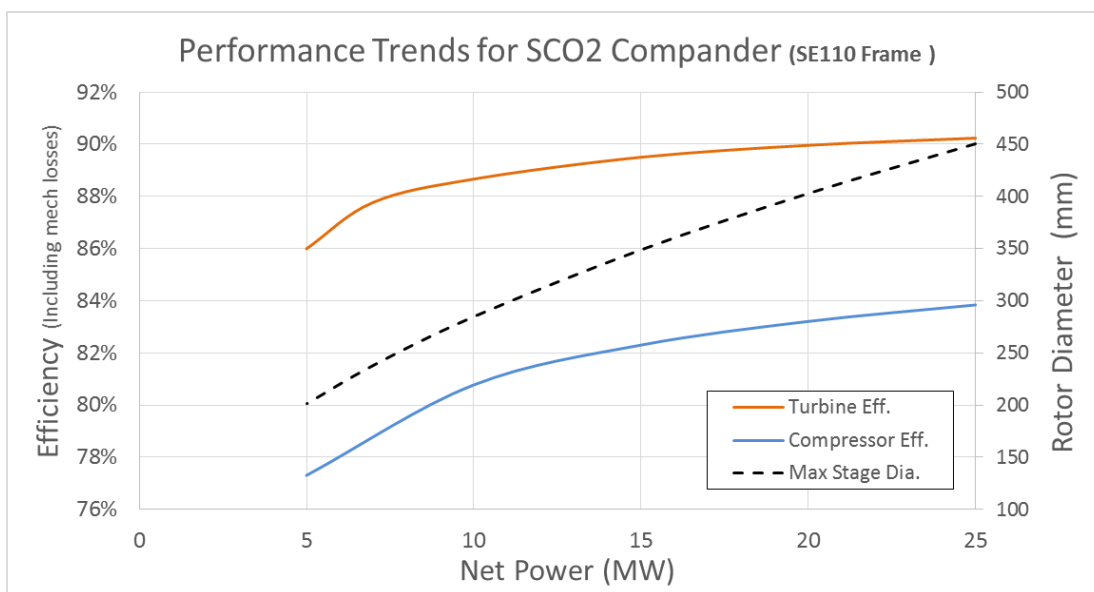
Figure 13: Performance of the SE110 compander operating in $_sCO_2$ at across a range of powers

Cycle Integration

Re-heating and intercooling improve the overall cycle efficiency when a recuperator is present in the power block. The modular configuration of the compander also allows for both intercooling and re-heating to be easily incorporated. Intercooling allows for a significant reduction in compression work to be achieved by cooling the inlet to the second stage for cases with a high pressure ratio. In the same way that intercooling can be applied to the compressors, re-heating can also be integrated with the turbine stages. Re-heating is achieved by incorporating a heat-exchanger between the turbine stages to add additional thermal energy to the fluid. Re-heating helps maximize the power output of the turbine and maximize the isothermal efficiency of the overall cycle as is done in most commercial gas-fired power plants. The additional efficiency associated with intercooling and re-heating does come at an additional cost, so the size and number of additional heat exchangers must be carefully considered against the overall power block cost targets of this project.

Mechanical Design

The detailed mechanical design of the core must meet the required aerodynamic performance and be safe and reliable. Several unique design features will be incorporated to accommodate the high temperatures and pressures of the working fluid. Figure 14 shows several of these key features. First, between each turbine casing and the main gearbox, an insulating plate will be used to separate the hot casing from the volute and protect the bearings. Second, high-strength casings will be designed following ASME pressure vessel guidelines to give robust management of the high pressure gas. The gearbox can also accommodate either dry gas or carbon ring seals. Dry gas seals will most likely be required for the turbine stages where the temperature or pressure is greatest. Carbon ring seals could be considered as an option for the lower temperature and pressure compressor stages. The covered impellers will be manufactured using advanced 3D metal printing. The 3D printed impellers will not have a shroud joint and will have minimal flow-path geometry limitations. The

detailed blade design leverages this technology to create a flow path that is both efficient and manages the high stresses.
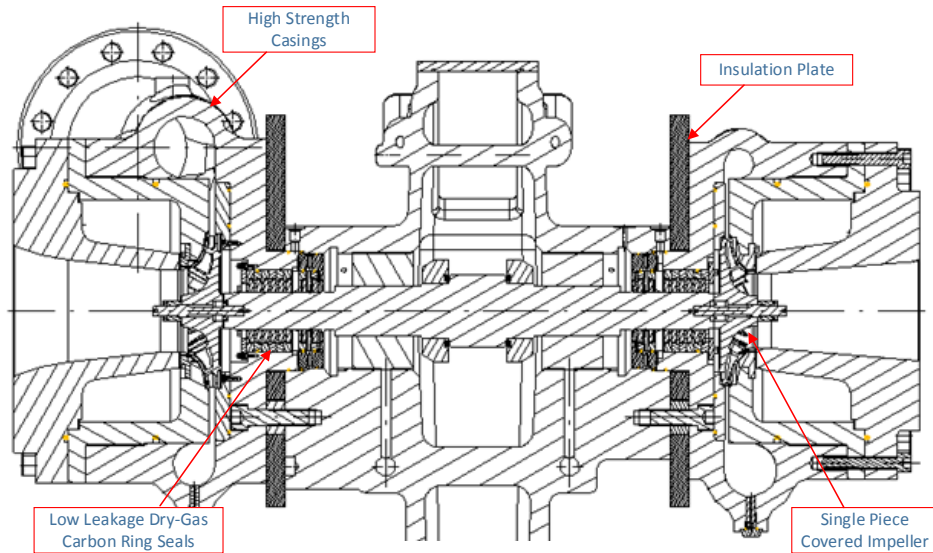
Figure 14: Cross-section of a single pinion showing key components

Performance

Preliminary sizing suggests that the turbines will have low aerodynamic performance risk since they will be sized near an optimal specific speed (~0.5) for radial inflow turbines. The greatest risk for the turbines will be mechanical limitations resulting from to creep at the high inlet temperatures. This risk is most easily mitigated by manufacturing the turbines with a material that is known to have acceptable creep strength and corrosion resistance, but limits on tip speed are expected. The compressor design will focus on maximizing the stable operating range to manage potential variations in the inlet state of the gas. Even in cases where the inlet temperature is above the saturation line, there is still a risk for large variations in properties and potential condensate formation due to a drop in static temperature and pressure that occurs in the compressor inlet. Table 8 below shows the non-dimensional sizing of the eight stages which are expected to comprise the machine.

Table 8: Aerodynamic Performance Summary

	Compressor				Turbine			
	Main Compressor		Re-compressor		HP Pinion		LP Pinion	
	Stage1	Stage2	Stage 1	Stage 2	Stage1	Stage2	Stage 3	Stage 4
Flow Coeff.	0.055	0.030	0.028	0.014	0.255	0.236	0.252	0.225
Head Coeff.	1.020	0.980	1.000	0.960	0.907	0.907	0.907	0.907
Specific Speed	0.691	0.520	0.502	0.368	0.425	0.400	0.400	0.354
Machine Mach #	0.985	0.581	1.029	0.961	0.399	0.449	0.519	0.633

CONCLUSION

This paper presents an interesting concept for a turbomachinery power block that is currently being applied to a supercritical CO2 power cycle for concentrating solar power technologies. This concept utilizes a compander to comprise the turbomachinery on the power block, which has a number of interesting features that can be leveraged to improve overall power-block efficiency. The study shows that optimizing thermodynamic efficiency for the given cycle requires the use of a single stage of turbine reheating, which can easily be accommodated on an integrally-geared machine. Additionally, simulations show that achieving an optimal efficiency will require fairly sophisticated control strategies, as the cycle pressure ratio, flow split, and use of compressor intercooling, are all heavily influential on cycle efficiency. Along with these control strategies, the compressor flow requirements have been found in the current work to be very demanding, requiring up to 55% for the main compressor and 35% for the recompressor [20].

REFERENCES

[1] Turchi, C., Mehos, M., Ho, C., & Kolb, G., "Current and Future Costs for Parabolic Trough and Power Tower Systems in the US Market," National Renewable Energy Laboratory, Sandia National Laboratories, Presented at SolarPACES 2010, September 21-24, 2010, Perpignan, France

[2] U.S. Department of Energy, "SunShot Vision Study," February, 2012, DOE/GO-102012-3037, Prepared by National Renewable Energy Laboratory, Accessed 2015, http://www1.eere.energy.gov/solar/pdfs/47927.pdf

[3] Turchi, C., & Heath, G., "Molten Salt Power Tower Cost Model for the System Advisor Model (SAM)," National Renewable Energy Laboratory, Colorado, 2013, http://www.nrel.gov/docs/fy13osti/57625.pdf

[4] System Advisor Model Version 2015.6.30 (SAM 2015.6.30), National Renewable Energy Laboratory, Golden, Colorado, Accessed, 2015, https://sam.nrel.gov/content/downloads

[5] Dyreby, J., Klein, S., Nellis, G., & Reindl, D., "Design Considerations for Supercritical Carbon Dioxide Brayton Cycles With Recompression," Journal of Engineering for Gas Turbines and Power, ASME, Vol. 136, Issue 10, 2014, pp. 101701

[6] Neises, T. and C. Turchi, "Supercritical CO_2 Power Cycles: Design Considerations for Concentrating Solar Power," The 4th International Symposium – Supercritical CO_2 Power Cycles, September 9-10, 2014, Pittsburgh, PA.

[7] Sarkar, J. and S. Bhattacharyya, "Optimization of recompression s-CO_2 power cycle with reheating," Energy Conversion and Management 50, 2009, p. 1939-1945.

[8] Turchi, Craig S., et al. "Thermodynamic study of advanced supercritical carbon dioxide power cycles for concentrating solar power systems." *Journal of Solar Energy Engineering* 135.4 (2013): 041007.

[9] Incropera, F. P., Dewitt, D., Bergman, T., & Lavine, A. Fundamentals of heat and mass transfer. 2007, Hoboken.

[10] Moore, J., & Musgrove G., "Performance and Cost Targets for sCO$_2$ Heat Exchangers," Panel Session, NETL-EPRI Workshop on Heat Exchangers for Supercritical CO$_2$ Power Cycles, October 15, 2015, San Diego, CA.

[11] Natural Gas Prices: Long Term Forecast to 2020, http://knoema.com/ncszerf/natural-gas-prices-long-term-forecast-to-2020-data-and-charts

[12] 2014, Department of Energy, Office of Energy Efficiency and Renewable Energy, "Concentrating Solar Power: Advanced Projects Offering Low LCOE Opportunities," FOA Number DE-FOA-0001186, CFDA No. 81.087

[13] U.S. Department of Energy, "President Requests $842.1 Million for Fossil Energy Programs," http://energy.gov/fe/articles/president-requests-8421-million-fossil-energy-programs.

[14] EIA Natural Gas Weekly Update http://www.eia.gov/naturalgas/weekly/#tabs-prices-3.

[15] Carbon Dioxide Emissions Coefficients, U.S. Energy Information Administration, 2013, https://www.eia.gov/environment/emissions/co2_vol_mass.cfm.

[16] Numerical Propulsion System Simulation (NPSS), http://www.swri.org/npss/.

[17] Fact Sheet: Carbon Pricing around the World, Environmental and Energy Study Institute, October 17, 2012, http://www.eesi.org/papers/view/fact-sheet-carbon-pricing-around-the-world?/fact-sheet-carbon-pricing-around-world-17-oct-2012.

[18] NIST REFPROP - http://www.nist.gov/srd/nist23.cfm.

[19] Neises, T. and C. Turchi, "Supercritical CO$_2$ Power Cycles: Design Considerations for Concentrating Solar Power," The 4th International Symposium – Supercritical CO$_2$ Power Cycles, September 9-10, 2014, Pittsburgh, PA.

[20] Allison, T., Wilkes, J., Pelton, R., and Wygant, K., 2016, "Conceptual Development of a Wide-Range Compressor Impeller for sCO$_2$ Applications," *5th Intl. Symposium – Supercritical CO2 Power Cycles*, Short Paper, March 28-31, San Antonio, TX.